



Spatial variations in sedimentary N-transformation rates in the North Sea (German Bight)

Alexander Bratek^{1,2}, Justus E. E. van Beusekom¹, Andreas Neumann¹, Tina Sanders¹, Jana Friedrich¹, Kay-Christian Emeis^{1,2}, and Kirstin Dähnke¹

¹Institute of Coastal Research, Helmholtz-Zentrum Geesthacht, Geesthacht, Germany

²Center for Earth System Research and Sustainability, Institute for Geology, University of Hamburg, Hamburg, Germany

Correspondence: Kirstin Dähnke (kirstin.daehnke@hzg.de)

Received: 27 July 2019 – Discussion started: 7 August 2019

Revised: 20 February 2020 – Accepted: 7 April 2020 – Published: 28 May 2020

Abstract. In this study, we investigate the role of sedimentary N cycling in the southern North Sea. We present a budget of ammonification, nitrification and sedimentary NO_3^- consumption and denitrification in contrasting sediment types of the German Bight (southern North Sea), including novel net ammonification rates. We incubated sediment cores from four representative locations in the German Bight (permeable, semi-permeable and impermeable sediments) with labeled nitrate and ammonium to calculate benthic fluxes of nitrate and ammonium and gross rates of ammonification and nitrification. Ammonium fluxes generally suggest oxic degradation of organic matter, but elevated fluxes at one sampling site point towards the importance of bioirrigation or short-term accumulation of organic matter. Sedimentary fluxes of dissolved inorganic nitrogen are an important source for primary producers in the water column, supporting $\sim 7\%$ to 59% of the average annual primary production, depending on water depth.

We find that ammonification and oxygen penetration depth are the main drivers of sedimentary nitrification, but this nitrification is closely linked to denitrification. One-third of freshly produced nitrate in impermeable sediment and two-thirds in permeable sediment were reduced to N_2 . The semi-permeable and permeable sediments are responsible for $\sim 68\%$ of the total benthic N_2 production rates, which, based solely on our data, amounts to $\sim 1030 \text{ t N d}^{-1}$ in the southern North Sea. Thus, we conclude that semi-permeable and permeable sediments are the main sinks of reactive N, counteracting eutrophication in the southern North Sea (German Bight).

1 Introduction

The continental shelves and coastal margins make up for $< 9\%$ of the total area of ocean surface but are responsible for vast majority of the biogeochemical cycling both in the water column and in the sediments (Jorgensen, 1983). For instance, 30% of global marine primary production occurs in coastal, estuarine and shelf systems (LOICZ, 1995), and nutrient regulation in shelf sediments is a particularly valuable ecosystem service (Costanza et al., 1997).

The German Bight is part of the southern North Sea, is bordered by densely populated and industrialized countries, and receives large amounts of nutrients via river discharge (e.g., Rhine, Maas, Elbe, Weser, Ems) (Los et al., 2014). This caused clear eutrophication symptoms such as phytoplankton blooms, oxygen deficiencies and macrobenthos kills especially during the 1980s (Hickel et al., 1993; von Westernhagen et al., 1986) in the North Sea. In the adjacent Wadden Sea intense phytoplankton blooms, a possible decrease in seagrass and massive blooms of opportunistic macroalgae were attributed to eutrophication (e.g., Cadée and Hegemann, 2002). Since the mid-1980s, the nitrogen (N) loads into the German Bight have been decreasing, but the entire SE North Sea is still flagged as an eutrophication problem area (OSPAR, 2010).

Nitrogen availability increases primary production on a variety of spatial and temporal scales. At present, major nitrogen sources for the southern North Sea are agricultural and urban waste water and, to a lesser extent, a variety of reactive N emissions (e.g., nitrogen oxides from burning fossil) (Emeis et al., 2015).

Internal N cycling in sediments (e.g., assimilation, ammonification and nitrification) changes the distribution and speciation of fixed N but not the overall amount of N available for primary production (Casciotti, 2016). Reduction of reactive nitrogen through denitrification and anammox in anoxic conditions back to unreactive N₂, however, does remove N from the biogeochemical cycle (Neumann et al., 2017).

Because these eliminating processes are confined to suboxic and anoxic conditions, they only occur in sediments in the generally oxygenated North Sea. Due to its putative relevance as an ecosystem service, denitrification has been subject to many studies, but ammonification as a source of N to primary production has so far received much less attention. This is in part due to the complexity created by coupled ammonification–nitrification in which different N processes, such as assimilation and denitrification, interact and affect the NH₄⁺ and NO₃⁻ concentrations in pore waters. To our knowledge, no ammonification rates in the North Sea have been quantified, whereas nitrification rates in permeable sediments were found to be on the same order of magnitude as denitrification rates (< 0.1 to ~ 3.0 mmol m⁻² d⁻¹; Table 1) (Marchant et al., 2016). N loss in the German Bight has been studied by several authors (e.g., Deek et al., 2013), showing high spatial, temporal and seasonal variability.

The main N loss process in the North Sea is denitrification, whereas anammox plays a minor role (Bale et al., 2014; Marchant et al., 2016). The main drivers of denitrification are organic matter content and permeability of the sediment (Neumann, 2012), and recent studies suggest that permeable sediments account for about 90 % of the total benthic NO₃⁻ consumption in the German Bight (Neumann et al., 2017).

Quantifying N dynamics based solely on changes in N concentrations provides limited insight into underlying reactions, as only net changes can be observed. Previous authors used different methods for determination of specific N rates. Lohse et al. (1993) used the acetylene block method, core flux incubations and isotope pairing in types of the early 1990s to determine denitrification rates in a variety of sediment types (Table 1). Deek et al. (2013, 2011) investigated N turnover in the Wadden Sea and in the extended Elbe estuary using core flux incubations and isotope pairing. Marchant et al. (2016) measured denitrification rates in permeable sediments obtained from slurry incubations and percolated sediment cores. More recently, Neumann et al. (2017) used pore-water NO₃⁻ concentration gradient profiles to determine NO₃⁻ consumption rates in the German Bight.

Stable isotope techniques offer several approaches to quantify N turnover processes, and ¹⁵N tracer studies have been widely used to determine N-transformation rates (e.g., nitrification and denitrification) (Brase et al., 2018; Sanders et al., 2018). The isotope dilution method can be used to distinguish between net and gross rates and so help to unravel several N processes, such as ammonification and assimilation or nitrification and denitrification. ¹⁵N dilution

(Koike and Hattori, 1978; Nishio et al., 2001) can be used to estimate gross N-transformation rates by measuring the isotopic dilution of the substrate and product pools (e.g., Burger and Jackson, 2003). In this study, we used the isotope dilution method with labeled NH₄⁺ and NO₃⁻ in separate sediment cores to measure gross ammonification and gross nitrification. The net rates are determined by the sediment nutrient fluxes. To measure denitrification, we determined the produced N₂ independently of the labeling in the core. The sediment core incubation experiment setup can never reproduce the identical conditions related to the advective processes in permeable sediments. Nevertheless this method has advantages over just balancing sediment–water exchanges: (1) the appearance of ¹⁵N in the NH₄⁺ pool during the incubation allows an estimate of ammonification rates, and (2) the isotopic dilution of NO₃⁻ tracks nitrification rates.

This study is conducted within the project North Sea Observation and Assessment of Habitats (NOAH). One important aspect of the project is to investigate the biogeochemical status and functions of the sea floor, especially nitrogen cycling, to gauge the eutrophication mitigation potential in light of continuing high human pressures (<https://www.noah-project.de>, last access: 17 May 2020).

In this paper, we investigate internal N rates of ammonification, nitrification and denitrification at four stations across sediment types (clay–silt, fine sand, coarse sand) in the German Bight (North Sea) during late summer (August–September) 2016. To assess the internal sediment N processes and the rates of reactive N release to the water column, we incubated sediment cores amended with ¹⁵NH₄⁺ and ¹⁵NO₃⁻. We quantify the benthic gross and net nitrification and ammonification rates and evaluate the environmental controls underlying spatial variabilities. We further discuss the role of ammonification as a source of reactive nitrogen for primary producers, of nitrification and of denitrification in the southern North Sea.

2 Material and methods

2.1 Study site and sampling strategy

The study site is in the German Bight (southern North Sea), an area that is strongly influenced by nutrient inputs from large continental rivers. The salinity in the coastal zone of the North Sea ranges between ~ 30 and 35, and the average flushing time is 33 d (Lenhart and Pohlmann, 1997). The sampling was performed in August and September 2016 during R/V *Heincke* cruise HE 471 in the German Bight (Fig. 1).

The sampling sites are part of the NOAH assessment scheme (Fig. 1). Samples were taken from four sites (NOAH-A, NOAH-C, NOAH-D and NOAH-E) with different water depth and sediment characteristics (Table 2). The sites represent typical sediment types based on statistics of granulometric properties, organic matter content, permeability

Table 1. Rates of nitrification, dissimilatory nitrogen reduction to ammonia (DNRA), anaerobic ammonia oxidation (anammox) and denitrification (DNIT) (in $\mu\text{mol N m}^{-2} \text{d}^{-1}$) in the North Sea of other published data.

Location	Nitrification	DNRA	Anammox	DNIT rate/ NO ₃ ⁻ uptake	Sediment type	C _{org}	C : N time	Sampling	Method	Reference
	(μmol m ⁻² d ⁻¹)				(-)	(% dry wt)	(atom)			(-)
German Bight (North Sea)	1233 ± 12	N.D.	N.D.	1314 ± 1087 ^a	Medium sand	0.03	< 0.01	August/ September 2016	SIDM	This study
	1739 ± 695	N.D.	N.D.	1355 ± 876	Fine sand	0.04	0.01			
	1271	N.D.	N.D.	1306 ± 1042		0.21	0.03			
	2069 ± 63	N.D.	N.D.	1915 ± 831		Clay/silt	0.73			
Dutch coast	N.D.	N.D.	0.0 0.2 1.3 0.6	N.D.	Fine sand	0.03	N.D.	November 2010 February 2011 May 2011 August 2011		
Oyster Ground	N.D.	N.D.	0.0 2.3 10.4 12.8	N.D.	Muddy sand/ clay/ silt	0.30	N.D.	November 2010 February 2011 May 2011 August 2011	SSI	Bale et al. (2014)
North Dogger	N.D.	N.D.	0.0 0.8 0.0 1.1	N.D.	Fine sand	0.03	N.D.	November 2010 February 2011 May 2011 August 2011		
Elbe estuary coastal zones	N.D.	N.D.	N.D.	771 ^a	Coarse sand	0.6	6.0	March 2009	IPT	Deek et al. (2013)
				1215 ^a		0.1	N.D.			
				3200 ^a		0.1	N.D.			
				864 ^a		0.6	6.0			
				1425 ^a 47 ^a 140 ^a		0.2 0.1 0.2	N.D.	September 2009		
Oyster Ground	288 ± 144 19 ± 96	N.D.	N.D.	12.0 ^a 19.2 ^a	Muddy sand	0.12	6.0	August 1991 February 1992		
Weiss Bank	216 120 ± 120			21.6 ^a 16.8 ^a	Fine sand	0.16	8.0	August 1991 February 1992		
Tail End	432 ± 168 264 ± 120			2.4 ^a 0 ^a		0.16	5.3	August 1991 February 1992		
Esbjerg	408 ± 216 168 ± 168			9.6 ^a 91.2 ^a	Silt	0.06	6.0	August 1991 February 1992		
Helgoland	0 216 ± 1220			45.6 ^a 196.8 ^a		1.28	8.5	August 1991 February 1992		
Elbe Rinne	264 ± 72 288 ± 96			4.8 ^a 31.2 ^a	Muddy sand	0.46	9.2	August 1991 February 1992		
Frisian Front	624 ± 288 192 ± 72			16.8 ^a 24.0 ^a	Coarse sand	0.46	9.2	August 1991 February 1992		
Sylt	81.6 ± 64.8 11 ± 2			372 ± 132 ^a 44.5 ± 13.5 ^a		0.12	6.0	June 1993 April 1994		
	3.8 ± 1.6			17 ± 4 ^a		N.D.	N.D.	April 1994		
	1116 ± 924 19.5 ± 9.5			75 ± 39 ^a 103.5 ± 17.5 ^a	Muddy sand		March 1993 April 1994			
Helgoland	1150 ± 700 210 ± 50	20 ± 5 250 ± 50	N.D.	870 ± 100 ^a 2280 ± 300 ^a	Fine sand Medium sand	N.D.	N.D.	May 2012	SIDM	Marchant et al. (2016)
	2980 ± 420	110 ± 60		520 ± 30 ^a	Coarse sand					
Sean Gras			24.0	48 ^a	Medium sand	0.05	8.1	April 2007		
			24.0	72 ^a		0.06	7.4	May 2007		
			0	120 ^a		0.10	8.5	September 2007		
			48.0	144 ^a		0.05	6.6	October 2007		
			0	24 ^a		N.D.	N.D.	April 2008		
Oyster Ground	N.D.	N.D.	24	288 ^a	Muddy sand	0.28	10.2	February 2007	IPT	Neubacher et al. (2011)
			24	120 ^a		0.22	9.0	April 2007		
			24	120 ^a		0.20	8.4	May 2007		
			120	408 ^a		0.22	9.2	September 2007		
			144	504 ^a		0.23	9.4	October 2007		
48	144 ^a	0.27	8.7	April 2008						
North Dogger			0	24 ^a	Muddy sand	0.45	10.2	February 2007		
			0	96 ^a		0.45	9.4	April 2007		
			24	168 ^a		0.42	9.7	May 2007		
			48	288 ^a		0.46	9.7	September 2007		
			48	264 ^a		0.38	9.6	October 2007		
German Bight/ Dogger Bank	N.D.	N.D.	N.D.	20.5 ± 4.5 ^b 28.5 ± 23.5 ^b	Mud	0.37 ± 0.02 0.16 ± 0.12		May 2009 February 2010		
				8 ± 8 ^b 12.5 ± 12.5 ^b	Muddy sand	0.13 ± 0.10 0.10 ± 0.08	N.D.	May 2009 February 2010	PWMF	Neumann et al. (2017)
				59.5 ± 25.5 ^b 99 ± 35.0 ^b	Sand	0.16 ± 0.13 0.02		May 2009 February 2010		

N.D. – not determined. ^a Denitrification. ^b NO₃⁻ uptake. Abbreviation of methods: SIDM – sediment isotope dilution method, MABT – modified acetylene block technique, SSI – sediment slurry incubations, PWMF – pore-water mean fitting – and IPT – isotope-pairing technique.

Table 2. Characteristics of bottom water and sediment characteristics of the sampled stations in the North Sea (<https://doi.org/10.1594/PANGAEA.846041>, last access: 17 May 2020). C_{org} means organic carbon content, TN means total nitrogen content of the surface sediment and OPD means oxygen penetration depth in the sediment.

Location (–)	Depth (m)	Sediment core (–)	Incubation time (h)	Sediment type (–)	C_{org} (%)	TN	Porosity (–)	Permeability (m^2)	Temp. ($^{\circ}C$)	Salinity (–)	OPD (mm)
NOAH-A	31.0	1	24	Medium	0.03*	$\leq 0.01^*$	0.37	1.7×10^{-10}	19.1	33.7	> 15
		2	24	sand							
		3	18								
		4	24								
NOAH-C	25.4	1	24	Clay/	0.73	0.10	0.56	1×10^{-15}	19.1	32.5	3.6
		2	24	silt							
		3	24								
NOAH-D	38.0	1	18	Fine	0.21	0.03	0.43	1.4×10^{-13}	18.9	33.0	2.4
		2	24	sand							
		3	24								
NOAH-E	28.4	1	18	Medium	0.04	0.01	0.41	8.8×10^{-12}	18.7	32.4	4.2
		2	18	sand							
		3	24								
		4	24								

* estimated.

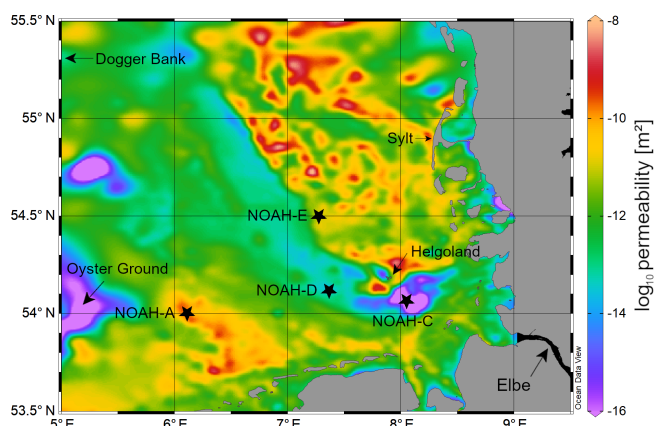


Figure 1. Map showing the sampling stations NOAH-A, NOAH-C, NOAH-D and NOAH-E in the German Bight in the North Sea. Colored areas show the spatial variability in surface sediment permeability (<https://doi.org/10.1594/PANGAEA.872712>, last access: 17 May 2020).

and water depth assessed during former cruises (<https://doi.org/10.1594/PANGAEA.846041>, last access: 17 May 2020). Organic matter and C/N ratio data from cruises HE 383 (July 2012) and HE 447 (June 2015) were used.

2.2 Core sampling and incubation

At each station (NOAH-A, NOAH-C, NOAH-D and NOAH-E) both water samples and sediment samples were taken. Water samples were taken with Niskin bottles attached to a CTD with additional chlorophyll and O_2 sensors. Sedi-

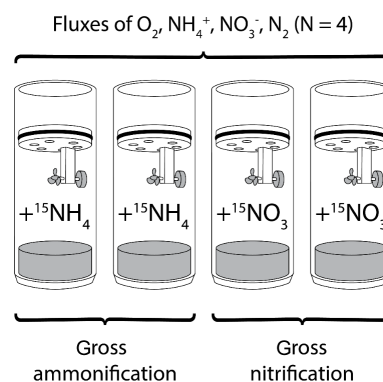


Figure 2. Schematic illustration of the experimental setup. Four sediment cores were incubated to measure benthic fluxes of oxygen, ammonium, nitrate and N_2 . Two of these flux cores were amended with either $^{15}NH_4^+$ or $^{15}NO_3^-$ for the measurement of gross rates of ammonification and nitrification, respectively.

ment multicores equipped with acrylic tubes (PMA) with an inner diameter of 10 cm and a length of 60 cm were used. Four intact sediment cores from each station (exception: at station NOAH-D, only three cores could successfully be retrieved) were incubated in a gas-tight batch-incubation setup for 24 h (Fig. 2) in the ship's laboratory at an in situ temperature ($\sim 19^{\circ}C$) directly after sampling. Cores were handled carefully to avoid disturbance that could alter benthic fluxes. Cores were incubated in the dark, and the overlying site water was gently stirred with a magnetic stirrer, avoiding sediment resuspension. The overlying water column was adjusted to a height of 20 cm. Water temperature and oxygen concentra-

tion of the overlying water of sediment cores were measured continuously with optodes (PyroScience, Germany).

To measure gross ammonification, two sediment cores (station NOAH-D: one core only) were enriched with $^{15}\text{NH}_4^+$ (50 at. %; the other two cores were amended with $^{15}\text{NO}_3^-$ (50 at. %) for an assessment of gross nitrification (Fig. 2). NH_4^+ and NO_3^- concentrations of the added tracer solution were adjusted to bottom water concentrations based on nutrient data of previous cruises of the same location and time (later confirmed by nutrient analyses of site water). For label addition, site water was replaced with the respective label solution. Due to the careful adjustment of concentrations, incubations were done at a tracer level, and benthic fluxes should not be altered. The label addition was calculated, aiming for a maximum enrichment of 5000‰ in substrates.

Samples were taken every 6 h. Upon sampling, incubation water was filtered with a syringe filter (cellulose acetate, Sartorius, 0.45 μm pore size) and frozen in Exetainers (11.8 mL, Labco, High Wycombe, UK) at -20°C for later analyses of nutrients and stable isotope signatures ($\delta^{15}\text{NH}_4^+$, $\delta^{15}\text{NO}_3^-$). Additional samples for the analyses of dissolved nitrogen (N_2) were taken without filtration and were preserved in Exetainers (5.9 mL, Labco, High Wycombe, UK) containing 2% of a ZnCl_2 solution (1 mol L^{-1}). Samples were stored at 4°C underwater until analysis.

2.3 Analyses

2.3.1 N_2 measurements by MIMS

N_2 production was measured by a membrane inlet mass spectrometer (MIMS; InProcess Instruments), which quantifies changes in dissolved N_2 : Ar ratios (Kana et al., 1994) from all four cores. During the measurements, the water samples were maintained in a temperature-controlled water bath (16°C). For calibration, we measured equilibrated water samples at four salinities, from 0 to 35 after each 10th water sample. We measured the production of ^{28}N . The internal precision of the samples was $< 0.05\%$ for N_2/Ar analyses.

2.3.2 Oxygen penetration depth

The oxygen penetration depth in the sediment of each station was measured using microoptodes (50 μm tip size; PreSens, Germany). The optodes were moved vertically into the sediment with a micromanipulator (PyroScience, Germany), in steps of 100–200 μm , depending on the oxygen concentration. Three O_2 profiles were measured in one sediment core of each station. The O_2 profiles were measured directly after core retrieval, i.e., within 10–15 min.

2.3.3 Sediment samples

The surface sediment samples (first 1 cm) of the cruises HE 383 (June–July 2012) and HE 447 (June 2015) were analyzed for total carbon and total nitrogen contents with an

elemental analyzer (Carlo Erba, NA 1500) The total organic carbon content was analyzed after removal of inorganic carbon using 1 mol L^{-1} hydrochloric acid. The standard deviation of sediment samples was better than 0.6% for C_{org} and 0.08% for N determination.

Permeability and porosity of the sediments were conducted with sediments from the cruise HE 471, and the methods were described in detail elsewhere (Neumann, 2016).

2.3.4 Dissolved inorganic nitrogen concentrations

NO_x , NO_2^- and NH_4^+ concentrations of the water-column samples were determined in replicate with a continuous flow analyzer (AA3, Seal Analytical, Germany) according to standard colorimetric techniques (NO_x , NO_2^- : Grasshoff et al., 1999; NH_4^+ : K  rouel and Aminot, 1997). NO_3^- concentration was calculated by difference between NO_x and NO_2^- . Based on replicate analyses, measurement precision for NO_x and NO_2^- was better than 0.1 $\mu\text{mol L}^{-1}$ and better than 0.2 $\mu\text{mol L}^{-1}$ for NH_4^+ .

Water samples from core incubations were analyzed in duplicate for concentrations of NH_4^+ , NO_2^- and NO_3^- using a multimode microplate reader, Infinite F200 Pro, and standard colorimetric techniques (Grasshoff et al., 1999) at the ZMT, Bremen. The standard deviations were $< 1 \mu\text{mol L}^{-1}$ for NO_3^- , $< 0.2 \mu\text{mol L}^{-1}$ for NO_2^- and $< 0.5 \mu\text{mol L}^{-1}$ for NH_4^+ .

2.3.5 Nitrogen isotope analyses

The nitrogen isotope ratios of NO_3^- were determined via the denitrifier method (Casciotti et al., 2002; Sigman et al., 2001). This method is based on the mass spectrometric measurement of isotopic ratios of N_2O produced by the bacterium *Pseudomonas aureofaciens*. Briefly, 20 nmol of sample NO_3^- was injected in a 20 mL vial containing Milli-Q water. Two international standards were used (IAEA NO_3^- $\delta^{15}\text{N} = +4.7\%$, USGS34 $\delta^{15}\text{N} = -1.8\%$) for a regression-based correction of isotope values. For further quality assurance, an internal standard was measured with each batch of samples. The standard deviation for $\delta^{15}\text{N}$ was better than 0.2‰.

For ammonium isotope measurements, nitrite was removed by reduction with sulfamic acid (Granger and Sigman, 2009) before NH_4^+ was chemically oxidized to NO_2^- by hypobromite at $\text{pH} \sim 12$ and then reduced to N_2O using sodium azide (Zhang et al., 2007); 10 nmol of NH_4^+ was injected, and all samples with $[\text{NH}_4^+] < 1 \mu\text{mol L}^{-1}$ were analyzed. For the calibration of the ammonium isotopes, we used three international standards (IAEA N1 $\delta^{15}\text{N} = +0.4\%$, USGS25 $\delta^{15}\text{N} = -30.4\%$, USGS26 $\delta^{15}\text{N} = +53.7\%$). The standard deviations were better than 1‰.

N_2O produced either by the denitrifier method or by the chemical conversion of ammonium was analyzed with a Gas-Bench II, coupled to an isotope ratio mass spectrometer (Delta Plus XP, Thermo Fisher Scientific).

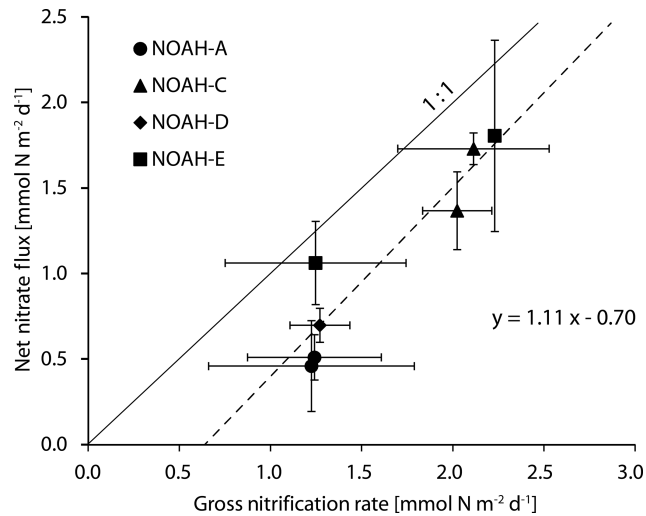


Figure 3. Correlation of gross nitrification rates and actual nitrate fluxes. The solid line indicates the 1 : 1 ratio, and the dashed line indicates the linear regression. The error bars indicate the regression error of individual rates at the 0.95 confidence level.

2.4 Rates and fluxes calculation for respiration, ammonification, nitrification and denitrification rates in core incubations

2.4.1 Benthic fluxes

Oxygen consumption, net ammonification, net nitrification and denitrification were calculated based on concentration changes in the sediment incubations. The respective benthic fluxes were calculated as follows:

$$r_{\text{net}} = d(C) \times V/d(t) \times A [\text{mmol N m}^{-2} \text{d}^{-1}], \quad (1)$$

where $d(C)$ is the oxygen, nutrient or nitrogen (N_2) concentration at the start and at the end of the experiment; V is the volume of the overlying water; $d(t)$ is the incubation time; and A is the surface area of the sediment. Positive fluxes (outflow concentrations above inflow concentrations) imply net production in the sediment.

2.4.2 Gross rates of ammonification and nitrification

Gross rates of ammonification and nitrification (r_{gross}) were calculated based on ^{15}N isotope dilution (Koike and Hattori, 1978; Nishio et al., 2001). For example, ammonification rates are calculated based on $^{15}\text{NH}_4^+$ additions, and nitrification rates are based on $^{15}\text{NO}_3^-$ additions (Fig. 2):

$$r_{\text{gross}} = \left[\ln \left(f^{15}\text{N}_{\text{end}} / f^{15}\text{N}_{\text{start}} \right) \right] / \left[\ln (C_{\text{end}} / C_{\text{start}}) \right] \times (C_{\text{start}} - C_{\text{end}} / t) \times (V/A \times \Delta t), \quad (2)$$

where C_{start} is the initial NH_4^+ or NO_3^- concentration, C_{end} is the concentration at time t , $f^{15}\text{N}_{\text{start}}$ and $f^{15}\text{N}_{\text{end}}$ represent

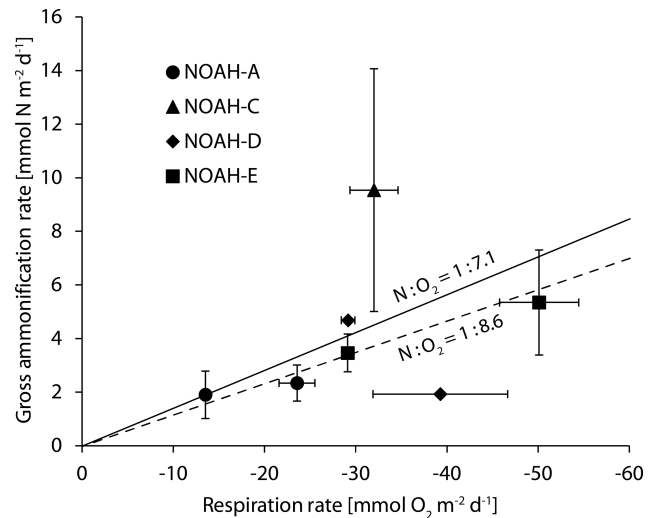


Figure 4. Benthic O_2 fluxes and gross ammonification rates of the sampled stations. The dashed line indicates the Redfield ratio of oxygen to nitrogen ($\text{N} : \text{O}_2$ 1 : 8625) (Redfield, 1958), and the solid lines indicate the ratio of oxygen to nitrogen determined by the C/N ratio in the North Sea ($\text{N} : \text{O}_2$ – 1 : 7.1). The error bars indicate the regression error of individual rates at the 0.95 confidence level.

^{15}N at. % excess (Brase et al., 2018), V is the volume of the overlying water, and A is the surface area of the sediment. (All rates are given in $\text{mmol N m}^{-2} \text{d}^{-1}$.)

3 Results

3.1 Ammonification

We measured gross ammonification rates with the isotope dilution method using $^{15}\text{NH}_4^+$ as tracer and measured net ammonium fluxes with the flux method. The highest net ammonium flux and gross ammonification rates were measured in the impermeable, organic-rich sediment at the station NOAH-C (6.6 ± 1.4 and $9.5 \text{ mmol N m}^{-2} \text{d}^{-1}$ for net flux and gross ammonification, respectively).

The lowest net ammonium fluxes were measured in the semi-impermeable sediment at the station NOAH-D ($0.5 \pm 0.1 \text{ mmol N m}^{-2} \text{d}^{-1}$). The lowest gross ammonification rate was measured at the permeable sediment station NOAH-A ($2.1 \pm 0.3 \text{ mmol N m}^{-2} \text{d}^{-1}$). The impermeable sediment station NOAH-C had the highest net ammonium fluxes ($6.6 \pm 1.4 \text{ mmol N m}^{-2} \text{d}^{-1}$) and gross ammonification rates ($9.5 \text{ mmol m}^{-2} \text{d}^{-1}$). Net and gross ammonification rates are significantly correlated ($r^2 = 0.55$; see Supplement).

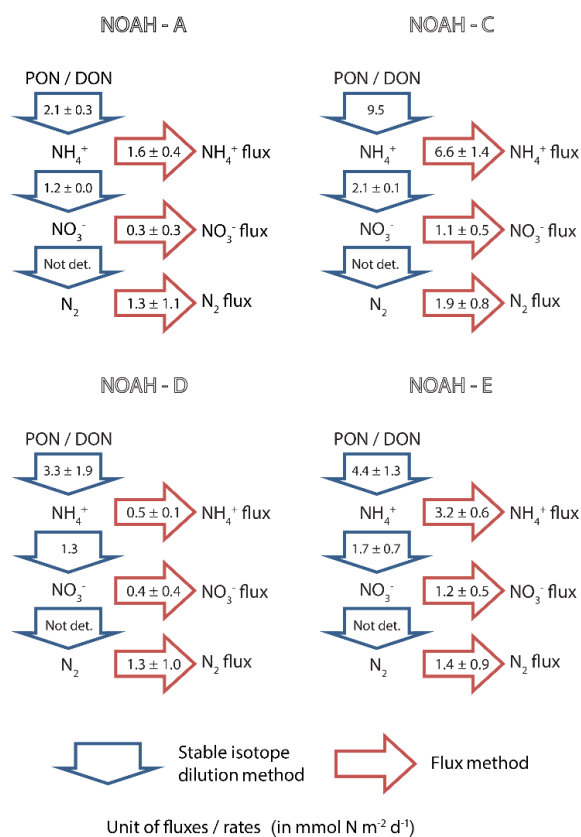


Figure 5. Benthic N-transformation rates (in mmol N m⁻² d⁻¹) of ammonification (NH₄⁺) and nitrification (NO₃⁻) as measured by means of stable isotope methods (blue arrows). Simultaneously measured fluxes of ammonium (NH₄⁺ flux), nitrate (NO₃⁻ flux) and N₂ (in mmol N m⁻² d⁻¹) as measured by the flux method (red arrows).

3.2 Nitrification

As for the ammonification, we measured gross nitrification rates by means of the stable isotope dilution method, with ¹⁵NO₃⁻ as tracer and net nitrate fluxes employing the flux method. Net fluxes and gross nitrification rates varied significantly between stations. Net nitrate fluxes were the highest at the station NOAH-C and at the station NOAH-E, with 1.1 ± 0.5 and 1.2 ± 0.5 mmol N m⁻² d⁻¹, respectively (Figs. 3, 5). Gross nitrification rates were the highest at NOAH-C (2.1 ± 0.1 mmol N m⁻² d⁻¹). The lowest rates of net nitrate flux (0.3 ± 0.3 mmol N m⁻² d⁻¹) and gross nitrification (1.2 ± 0.0 mmol N m⁻² d⁻¹) were observed in the permeable sediment at the station NOAH-A. Net and gross nitrification rates are closely correlated ($r^2 = 0.87$; Fig. 3), with net nitrate fluxes being systematically lower than gross nitrification rates.

3.3 Denitrification

Unlike ammonification and nitrification, we were not able to make use of the stable isotope tracers to evaluate N₂ production rates with a stable isotope technique because the requirements for the isotope-pairing method (Rysgaard-Petersen et al., 1996) were not met due to the labeled ¹⁵NO₃⁻ in the overlying water being too low to measure any ¹⁵N–N₂ species. Our N₂ production estimates are thus limited to the flux method. The observed average denitrification rates ranged from 1.3 ± 1.1 to 1.9 ± 0.8 mmol N m⁻² d⁻¹ (Fig. 5) and did not vary significantly between stations.

3.4 Sedimentary organic matter descriptions

The data show a clear correlation between sediment type and organic carbon and nitrogen content. Clay and silty sediment (NOAH-C) had the highest organic carbon (0.73 %) and nitrogen (0.10 %) concentrations (Table 2). The medium sand station (NOAH-A) had the lowest C_{org} (0.03 % to 0.04 %) and total nitrogen (< 0.01 % to 0.01 %) concentrations. This trend does probably not apply to NOAH-E, since the samples for C/N analyses were retrieved prior to the abrupt emergence of a large pockmark field at this station (Krämer et al. 2017), while the sediment cores for the incubations were retrieved after the emergence of the pockmarks. The large-scale sediment resuspension event resulted in numerous newly formed depressions with increased sedimentation of organic material.

4 Discussion

4.1 Magnitude and relevance of ammonification

A principal goal of this study was to assess the role of ammonification in the nitrogen cycle of the German Bight. Ammonification releases NH₄⁺ during the decomposition of organic matter and resupplies the water-column inventory of reactive nitrogen. The quantification of ammonification rates is challenging because ammonium is readily assimilated by primary producers or is rapidly nitrified, causing low ammonium concentrations and necessitating the use of the isotope dilution method.

This study represents direct measured gross ammonification rates across typical sediment types of the North Sea, covering a large range, from 1.9 to 9.5 mmol N m⁻² d⁻¹: ammonification rates were mainly governed by sediment texture and organic matter content. The impermeable muddy sediment at the station NOAH-C with high C_{org} and TN content (0.73 % and 0.10 %, respectively; Table 2) had the highest gross and net ammonification rates. This is line with other studies showing enhanced ammonium release in muddy coastal sediments (e.g., Caffrey, 1995).

The sandy sediments at sites NOAH-A, NOAH-D and NOAH-E exhibited significantly lower gross ammonification

rates. This reflects the lower sediment organic matter content in these sandy sediments, expressed in C_{org} (0.03 %–0.04 %) and N (0.01 %–< 0.01 %) concentrations (Caffrey, 1995; Table 2).

It is striking, though, that net and gross ammonification in the sandy sediment at the station NOAH-E was clearly elevated compared to the other sandy stations NOAH-A and NOAH-D. There are two possible explanations for this enhanced ammonium production: (1) enhanced supply of organic matter to the sediment surface or (2) effects of bioirrigation and bioturbation.

Station NOAH-E is located inside a pockmark field that had developed relatively recently, between July and November 2015 (Krämer et al., 2017). Our assessment of C and N content is based on samples that were taken prior to the pockmark formation in 2012 and 2015 (<https://doi.org/10.1594/PANGAEA.883199>, last access: 17 May 2020). The sediment samples during the cruise (HE 471) in 2016 were taken from the depression inside an individual pockmark, which was about ~ 0.2 deeper than the surrounding sediment (Krämer et al., 2017). We assume that organic matter from the water column accumulated in these transient structures and that the organic carbon and nitrogen content was thus elevated. A transient change in surface sediment composition, which is not captured by our compositional data, may thus have caused the enhanced ammonification rate.

An alternative explanation is an elevation of ammonium fluxes from the sediment due to sediment reworking. In the sediment incubations, we found high benthic activity of *Spiophanes bombyx* and *Phoronis* sp. Both benthic organisms can increase the nutrient fluxes from the sediment to the bottom water, the oxygen penetration depth and, in turn, organic matter degradation in the oxic zone (Aller, 1988).

Under completely oxic conditions, the ratio of NH_4^+ release to O_2 consumption in the entire study area should approximate Redfield ratios of about 1 : 8.6 (Thibodeau et al., 2010). Such ratios were observed at the semi-permeable station NOAH-D, at the permeable station NOAH-A (Fig. 2) and at the station NOAH-E, suggesting that in these cores most of the organic matter was degraded under oxic conditions. At station NOAH-C, however, the N: O_2 ratio was clearly elevated above the Redfield ratio. While this finding is based on an individual assessment, it appears plausible: we presume that the enhanced production of ammonium relative to O_2 consumption reflects the importance of anoxic ammonium generation, i.e., during methanogenesis or sulfate reduction (e.g., Jørgensen, 1982). This is quite likely at the station NOAH-C, where oxygen penetration depth in the impermeable, organic-rich sediment is the lowest and where increasing NH_4^+ concentrations with depth indicate decomposition or organic matter in the absence of free oxygen (Hartmann et al., 1973).

4.2 Ammonification coupled to denitrification by nitrification

Based on the interpolation of gross rates of ammonification, it is evident that ammonification contributes significantly to nutrient regeneration in the German Bight. However, there is a clear difference between gross and net ammonification rates, suggesting that ammonium is taken up, either by assimilation or by nitrification. In dark sediments, where phototrophic organisms are light limited, we presume that nitrification is likely the more important process (Dähnke et al., 2012).

Nitrification produces NO_3^- , which represents the largest DIN pool in the water column of the North Sea and is the substrate for denitrification and thus the link to an ultimate removal of fixed nitrogen from the water column.

We observed gross nitrification rates at all four stations, ranging from $1.2 \pm 0.0 \text{ mmol N m}^{-2} \text{ d}^{-1}$ at the sandy station NOAH-A to $1.3 \text{ mmol N m}^{-2} \text{ d}^{-1}$ in the moderately permeable sediment at NOAH-D and to $2.1 \pm 0.1 \text{ mmol N m}^{-2} \text{ d}^{-1}$ in the impermeable sediment at the station NOAH-C (Figs. 3, 5). Gross nitrification accounted for around 22.2 % (± 0.7 %) at the impermeable sediment station NOAH-C, around 38.5 % at the semi-permeable station (NOAH-D) and around 50.6 % (± 15.8 %) at the permeable sediment stations of total DIN flux to the bottom water. Overall, nitrification is in the same range as reported by Marchant et al. (2016) in sandy sediment near Helgoland (0.2 to $3.0 \text{ mmol m}^{-2} \text{ d}^{-1}$; Table 1). The highest nitrate fluxes from the sediment and gross nitrification rates were observed at the impermeable station NOAH-C and at the station NOAH-E, where pockmark structure and organic matter accumulation might have affected benthic nutrient fluxes (see Sect. 4.1).

The lowest gross nitrification rates and nitrate fluxes are found at the permeable station NOAH-A, but apart from this, we do not see a clear correlation of nitrification and permeability in our study. Nonetheless, nitrification rates are the lowest at the station NOAH-A, where oxygen penetration depth is the highest, and the sediment has low organic matter content (Table 2). A high oxygen penetration depth can support nitrification, but it is in this case obviously substrate limited due to low organic matter content, which limits ammonification. Oxygen penetration can enhance nitrification at greater depth but can, on the other hand, also increase diffusion limitation (Alkhatib et al., 2012).

Due to this dual control of nitrification by OPD on the one hand and substrate availability on the other hand, the individual correlations between C_{org} or TN and nitrification are relatively weak. Generally, organic matter deposition in the sediment supports higher ammonification rates, which in turn enhance nitrification under oxic conditions (Henriksen and Kemp, 1988; Rysgaard et al., 1996). Consequently, nitrification is affected by the NH_4^+ pool in the sediment, temperature, salinity and O_2 (e.g., Sanders, 2018).

This interplay of factors is mirrored in a clear and statistically significant ($\alpha = 0.05$) correlation of gross nitrification and gross ammonification rates ($r^2 = 0.92$). Overall, the gross NO_3^- production (1.2 to 2.1 $\text{mmol m}^{-2} \text{d}^{-1}$) was small relative to ammonification rates (1.9 to 9.5 $\text{mmol N m}^{-2} \text{d}^{-1}$). We find that nitrification is governed by a complex interplay of variables, such as ammonification rate, permeability, organic matter availability and oxygen penetration depth, and is likely difficult to predict based on one of these factors alone. Generally, organic matter deposition in the sediment supports higher ammonification rates, which in turn enhance nitrification under oxic conditions (Henriksen and Kemp, 1988; Rysgaard et al., 1996). In our setting, this is reflected in a clear correlation of gross rates of ammonification and nitrification.

4.3 Denitrification

Denitrification, the reduction of NO_3^- to gaseous N_2 , reduces the pool of bioavailable N and is therefore very relevant in eutrophic coastal areas such as the southern North Sea. In our study, the measured denitrification rates ranged from 1.3 to 1.9 $\text{mmol N m}^{-2} \text{d}^{-1}$ (Fig. 5). This estimate is on the higher end of previous measurements from sites in the German Bight (Deek et al., 2013; Marchant et al., 2016) (Table 1) but generally fits with previous observations. We assume that the rates in our study are elevated because sampling took place after the spring phytoplankton bloom, and not all organic matter that had been deposited at the sediment surface had been remineralized. Such a decoupling of water-column production and sedimentary denitrification has been observed before in stratified water masses of the Baltic Sea (Helleman et al., 2017). Even though our study was designed to cover diverse sediment types, and thus allow for an improved extrapolation of rates to the total German Bight area, this highlights the heterogeneity of sediments and points out that the sampling season can have a marked effect on measured rates. Therefore, follow-up experiments should try to cover the seasonality as much as possible to improve estimates of denitrification in the German Bight area.

Important seasonal effects on denitrification can be attributed to variations in oxygen supply, changing bottom water NO_3^- concentration and organic carbon content in the sediment (Deek et al., 2013). In our study, the bottom water nitrate concentration is too low (< 0.5 to $4.5 \mu\text{mol L}^{-1}$) to sustain the observed denitrification rates, and thus the major nitrate source fueling the observed denitrification must be coupled nitrification–denitrification fueled by mineralization of sedimentary organic material. This is reflected in a strong correlation between gross nitrification and denitrification rates ($r^2 = 0.85$).

In our study, we find that this coupled nitrification–denitrification determines the total N flux. Denitrification essentially removes, within the given uncertainties (Fig. 5), all nitrate produced by nitrification at study sites NOAH-A and

NOAH-D. At stations NOAH-C and NOAH-E, where we assume an (possibly transient in case of NOAH-E) accumulation of organic matter, nitrification rates are enhanced, and a substantial amount of freshly produced nitrate is released to the water column.

In comparison to the supply of mineralized N (i.e., gross ammonification), denitrification accounts for $\sim 20\%$ ($1.9 \text{ mmol N m}^{-2} \text{d}^{-1} / 9.5 \text{ mmol N m}^{-2} \text{d}^{-1}$) at the impermeable sediment station NOAH-C, $\sim 39\%$ ($1.3 \text{ mmol N m}^{-2} \text{d}^{-1} / 3.3 \text{ mmol N m}^{-2} \text{d}^{-1}$) at the semi-permeable sediment station NOAH-D and $\sim 62\%$ ($1.3 \text{ mmol N m}^{-2} \text{d}^{-1} / 2.1 \text{ mmol N m}^{-2} \text{d}^{-1}$) at permeable sediment stations (NOAH-A). As discussed above, this trend does not hold for the less representative station NOAH-E due to the transient formation of numerous pockmarks.

4.4 Significance of benthic N recycling

Our study covers the most sediment types across the German Bight but is based on core incubations and therefore potentially underestimates advective processes. In a recent study by Neumann et al. (2017), the authors used NO_3^- pore-water profiles to calculate the NO_3^- consumption rates across a similar range of North Sea sediments. They extrapolated their nitrate consumption rates to the entire area of the German Bight based on a permeability classification of sediments. They propose that $\sim 24\%$ of sediments in the southern North Sea (German Bight) are impermeable sediments ($12\,200 \text{ km}^{-2}$), $\sim 39\%$ are moderately permeable sediments ($19\,600 \text{ km}^{-2}$) and $\sim 37\%$ ($18\,800 \text{ km}^{-2}$) are permeable sediments. They estimated that permeable sediments were the most efficient NO_3^- sink, accounting for up to 90% of the total benthic NO_3^- consumption. In our assessment, which better represents the role of nitrification, we arrive at a somewhat lower contribution of $\sim 68\%$ of total denitrification occurring in moderately permeable and permeable sediments. Based solely on our data, we estimate a total nitrogen removal of $\sim 1030 \text{ t N d}^{-1}$ in our study area, which corresponds to an average N_2 flux of approximately $1.5 \text{ mmol N m}^{-2} \text{d}^{-1}$. This daily N_2 production during late summer equals the total N discharge ($\sim 1000 \text{ t N d}^{-1}$) by the main rivers, the Maas, Rhine, Ems, Weser and Elbe rivers, and the North Sea Canal (Pätsch and Lenhart, 2004) and, as such, underscores the role of coastal sediments to counteract the eutrophication in the North Sea.

Our assessment, however, does reflect the impact of only diffusive transport and faunal activity while not accounting for advective fluxes. Based on the same dataset of permeability for classification of different sediment types that Neumann et al. (2017) used, we merge our dataset with the results of Neumann et al. (in preparation) to arrive at an improved estimate of sediment denitrification that includes benthic nitrification as a nitrate source.

In the following, we aim to put our estimates of N-transformation rates into perspective by setting an upper

Table 3. Rates of benthic net NO_3^- and benthic net NH_4^+ fluxes per area, water depth below thermocline (average value of all sediment cores per station) and concentration of dissolved inorganic nitrogen (DIN) in the thermocline. Bottom water ($c\text{NO}_3^-$), nitrite ($c\text{NO}_2^-$) and ammonium ($c\text{NH}_4^+$). The concentration of DIN per area was calculated by the multiplication of the water depth below the thermocline with the concentration of DIN. Turnover rates of nitrogen were calculated by the division of DIN per area by the rates of NH_4^+ net and NO_3^- net and the effect of sedimentary N release on the reactive nitrogen available for primary production in the water column.

Station	$r\text{NH}_4^+_{\text{net}} + r\text{NO}_3^-_{\text{net}}$	Water depth below thermocline	$c\text{NO}_3^-$	$c\text{NO}_2^-$	$c\text{NH}_4^+$	DIN per area	N turnover	Sedimentary N support for primary production
(–)	($\text{mmol m}^{-2} \text{d}^{-1}$)	(m)	($\mu\text{mol L}^{-1}$)			(mmol m^{-2})	(days)	(%)
NOAH-A	1.6 ± 0.4	29.5	0.1	< 0.1	0.6 ± 0.2	20.7	10.8 ± 0.3	14.1 ± 4.7
NOAH-C	6.6 ± 1.4	10.0	< 0.1	0.7	2.0 ± 0.2	30.0	3.4 ± 0.1	58.7 ± 10.6
NOAH-D	0.5 ± 0.1	38.0	0.1 ± 0.1	0.1	0.8 ± 0.6	26.6	28.5 ± 0.6	7.1 ± 2.6
NOAH-E	3.2 ± 0.6	10.0	< 0.1	< 0.1	0.3 ± 0.1	3.0	0.9 ± 0.1	26.5 ± 14.3

limit of N turnover based on primary production, since N cycling is linked to organic carbon availability, which is ultimately provided by pelagic primary production. For the freshwater-influenced regions of the German Bight, Capuzzo et al. (2018) assume a C fixation of $1.05 \text{ g C m}^{-2} \text{d}^{-1}$. For an estimate of the maximum N-transformation rate we assume that 10 % of the fixed C is processed in the sediment (Heip et al., 1995) and that all carbon is remineralized in the sediment in pace with N turnover. Based on Redfield stoichiometry ($12 \text{ g mol}^{-1} \text{C}$, $\sim 14 \text{ g mol}^{-1} \text{N}$), average C fixation translates to $[1.05 \text{ g} \times 10 \% / 12 \text{ C} \times 14 \text{ N}] = 0.123 \text{ mg N m}^{-2} \text{d}^{-1}$ that is removed, or $9 \text{ mmol N m}^{-2} \text{d}^{-1}$, respectively. This sets an upper limit to the N turnover rate and compares well with the observed ammonification rate in impermeable sediment at NOAH-C ($9.5 \text{ mmol NH}_4^+ \text{ m}^{-2} \text{d}^{-1}$; Fig. 5). The ammonification rates at the sandy stations are substantially lower, which certainly reflects that sandy sediments are frequently resuspended and organic particles are resuspended and degraded in the water column. For a second line of argument, we consider the annual nitrate budget of the southern North Sea (Hydes et al. 1999; van Beusekom et al. 1999), with an annual average denitrification rate of $0.7 \text{ mmol N m}^{-2} \text{d}^{-1}$. This value agrees well with the average gap of $0.5 \text{ mmol N m}^{-2} \text{d}^{-1}$ between gross nitrification and actual nitrate flux (Fig. 4), which we attribute to denitrification. Both rates, the budget-based estimate and the nitrification gap, are in the lower range of our measured N_2 fluxes of 0.3 to $2.9 \text{ mmol N m}^{-1} \text{d}^{-1}$ (Table 1; Fig. 5). For a third line of argument, we employ the approach of Seitzinger and Giblin (1996) to link benthic respiration and denitrification directly to the pelagic primary production. By employing their formulas and using the primary production rates by Capuzzo et al. (2018), the annual average of the sediment oxygen demand would be $14.3 \text{ mmol O}_2 \text{ m}^{-2} \text{d}^{-1}$ ($1.05 \text{ g C d}^{-1} \text{ m}^{-2} = 87.5 \text{ mmol C d}^{-1} \text{ m}^{-2}$), which corresponds to a benthic denitrification rate of $3.3 \text{ mmol N m}^{-2} \text{d}^{-1}$. Since the annual average of actually measured oxygen fluxes is close to this estimate ($15.4 \pm 12.9 \text{ mmol O}_2 \text{ m}^{-2} \text{d}^{-1}$, $N = 175$) (Neumann et al.,

2020), we are confident that our denitrification estimates of up to $2.9 \text{ mmol N m}^{-2} \text{d}^{-1}$ are reasonable.

However, with the multitude of our approaches yielding quite a span of plausible denitrification estimates, the question emerges as to which of the figures in the range of 0.5 to $3.3 \text{ mmol N m}^{-1} \text{d}^{-1}$ is actually the true value for the average denitrification rate. One major reason for this level of uncertainty is the fact that the local sediment properties with regard to macrofauna composition and organic matter content varied considerably within each station, which is reflected, for example, in the variability in oxygen consumption rates (see Supplement). Since we were restricted to four cores per station in total, and just two cores for labeling with $^{15}\text{NH}_4^+$ and $^{15}\text{NO}_3^-$ the inevitable spatial heterogeneity introduced a substantial degree of random error. Additionally, the preceding results we used above to evaluate our observations are certainly likewise based on imperfect data, which results in uncertainty on that side. In summary, our limited set of new observations is not sufficiently large to favor one of the preceding denitrification estimates. At least, the average of all our N_2 measurements of $1.5 \pm 0.9 \text{ mmol N m}^{-2} \text{d}^{-1}$ ($N = 13$) falls right in the center of the interval of 0.5 to 3.3 mm and might represent our best estimate for an average denitrification rate in late summer. The remaining fraction of the initial ammonification is recycled back into the water column as DIN, which accounts for $69 \pm 18 \%$ ($N = 12$) of the total benthic N flux ($\text{N}_2 + \text{DIN}$).

Since benthic N recycling substantially restocks the pelagic N inventory, we further assessed the contribution of benthic N recycling by comparing the benthic DIN (ammonium + nitrite + nitrate) fluxes with the inventory of DIN below the thermocline. Assuming steady state, we find a rapid turnover of sediment-derived DIN at NOAH-C and NOAH-E, in the range of 1–3 d (Table 3). This implies that even below the thermocline, DIN derived by the sediment is rapidly assimilated by phytoplankton. Previous publications showed that primary production below the thermocline contributes $\sim 37 \%$ to total primary production in the North Sea (van Leeuwen et al., 2013). Assuming Redfield stoichiome-

try and an average primary production of $1.05 \text{ g C m}^{-2} \text{ d}^{-1}$, benthic DIN fluxes in our measurements can support a primary production of about 6.2 to $51.4 \text{ mmol C m}^{-2} \text{ d}^{-1}$ or $74\text{--}617 \text{ mg C m}^{-2} \text{ d}^{-1}$. This is within the range of previously observed and modeled primary production rates in the North Sea during summer (e.g., van Leeuwen et al., 2013). We further estimate that depending on the thickness of the bottom water layer below the thermocline, benthic N fluxes during the sampling time supported between $7.1 \pm 2.6 \%$ (38 m bottom water layer) and $58.7 \pm 10.6 \%$ (10 m bottom water layer) of the annual average of primary production (Table 3). This dependence of relative sediment contribution on water depth has been observed previously for respiration processes (Heip et al., 1995). Our data also match the calculation of Blackburn and Henriksen (1983) for Danish sediments, where N fluxes could support 30 % to 83 % of the nitrogen requirement of the planktonic primary producers (Blackburn and Henriksen, 1983).

5 Summary and concluding remarks

We evaluated a range of sedimentary nitrogen turnover pathways and found that ammonification in sediments is an important N source for primary production in the water column of the southeastern North Sea during summer. Depending on water depth, 7.1 % to 58.7 % of the estimated water-column primary production is fueled by sedimentary N release. Nitrification acts as the main sinks of NH_4^+ mineralized from sedimentary organic matter. Ultimately, the main factors governing nitrification are organic matter content and ammonification and oxygen penetration depth in the sediment. The share of newly produced NO_3^- reduced to N_2 amounts to two-thirds of NO_3^- in permeable sediments, to nearly one-half in moderately permeable sediment and to one-third in impermeable sediments. We further showed that moderately permeable and permeable sediments account for up to $\sim 80 \%$ of the total benthic N_2 production ($\sim 1030 \text{ t N d}^{-1}$) in the southern North Sea (German Bight) during the peak of benthic activity in late summer. Only then can benthic N_2 production compensate the annually averaged daily N input by the main rivers (e.g., Elbe, Ems, Rhine, Weser) discharging into the southern North Sea ($\sim 1000 \text{ t N d}^{-1}$). Thus impermeable sediments act as an important N source for primary producers, whereas moderately permeable and permeable sediments comprise a main reactive N sink counteracting eutrophication in the North Sea. Seasonal and spatial variabilities, especially from nearshore to offshore, should be evaluated in future studies.

Data availability. The data used in the present study are available in the Supplement.

Supplement. The supplement related to this article is available online at: <https://doi.org/10.5194/bg-17-2839-2020-supplement>.

Author contributions. AB, AN, TS and KD designed the research. AB carried out the fieldwork and performed the analyses. All authors interpreted the data. AB, AN, JvB, TS and KD wrote the paper, with comments provided by KCE and JF.

Competing interests. The authors declare that they have no conflict of interest.

Acknowledgements. We thank the captain and the crew of R/V *Heincke* for their support during the sampling campaigns. Matthias Birkicht from the Leibniz Centre for Tropical Marine Research (ZMT) in Bremen is gratefully acknowledged for his assistance with nutrient measurements. We further thank Ella Logemann for the analysis of macrobenthos. We also gratefully thank the two anonymous reviewers for comments that helped to greatly improve this paper.

Financial support. The article processing charges for this open-access publication were covered by a Research Centre of the Helmholtz Association.

Review statement. This paper was edited by Perran Cook and reviewed by two anonymous referees.

References

- Alkhatib, M., Lehmann, M. F., and del Giorgio, P. A.: The nitrogen isotope effect of benthic remineralization-nitrification-denitrification coupling in an estuarine environment, *Biogeosciences*, 9, 1633–1646, <https://doi.org/10.5194/bg-9-1633-2012>, 2012.
- Aller, R. C.: Benthic Fauna and Biogeochemical Processes in Marine Sediments: The Role of Burrows Structures, in: *Nitrogen cycling in Coastal Marine Environments*, edited by: Blackburn, T. H. and Sørensen, J., Scope, Chichester, 301–338, 1988.
- Bale, N. J., Villanueva, L., Fan, H., Stal, L. J., Hopmans, E. C., Schouten, S., and Sinninghe Damste, J. S.: Occurrence and activity of anammox bacteria in surface sediments of the southern North Sea, *FEMS Microbiol. Ecol.*, 89, 99–110, 2014.
- Blackburn, T. H. and Henriksen, K.: Nitrogen cycling in different types of sediments from Danish waters, *Limnol. Oceanogr.*, 28, 477–493, 1983.
- Brase, L., Sanders, T., and Daehnke, K.: Anthropogenic changes of nitrogen loads in a small river: external nutrient sources vs. internal turnover processes, *Isot. Environ. Health. S.*, 54, 168–184, 2018.

- Burger, M. and Jackson, L. E.: Microbial immobilization of ammonium and nitrate in relation to ammonification and nitrification rates in organic and conventional cropping systems, *Soil Biol. Biochem.*, 35, 29–36, 2003.
- Cadée, G. C. and Hegemann, J.: Phytoplankton in the Marsdiep at the end of the 20th century; 30 years monitoring biomass, primary production, and *Phaeocystis* blooms, *J. Sea Res.*, 48, 97–110, 2002.
- Caffrey, J. M.: Spatial and Seasonal Patterns in Sediment Nitrogen Remineralization and Ammonium Concentrations in San Francisco Bay, California, *Estuar. Coast. Shelf S.*, 18, 219–233, 1995.
- Capuzzo, E., Lynam, C. P., Barry, J., Stephens, D., Forster, R. M., Greenwood, N., McQuatters-Gollop, A., Silva, T., van Leeuwen, S. M., and Engelhard, G. H.: A decline in primary production in the North Sea over 25 years, associated with reductions in zooplankton abundance and fish stock recruitment, *Global Change Biol.*, 24, 352–364, 2018.
- Casciotti, K. L.: Nitrogen and Oxygen Isotopic Studies of the Marine Nitrogen Cycle, *Ann. Rev. Mar. Sci.*, 8, 379–407, 2016.
- Casciotti, K. L., Sigman, D. M., Hastings, M. G., Böhlke, J. K., and Hilkert, A.: Measurement of the oxygen isotopic composition of nitrate in seawater and freshwater using the denitrifier method, *Anal. Chem.*, 74, 4905–4912, 2002.
- Dähnke, K., Moneta, A., Veuger, B., Soetaert, K., and Middelburg, J. J.: Balance of assimilative and dissimilative nitrogen processes in a diatom-rich tidal flat sediment, *Biogeosciences*, 9, 4059–4070, <https://doi.org/10.5194/bg-9-4059-2012>, 2012.
- Deek, A., Dähnke, K., van Beusekom, J., Meyer, S., Voss, M., and Emeis, K.: N_2 fluxes in sediments of the Elbe Estuary and adjacent coastal zones, *Mar. Ecol. Prog. Ser.*, 493, 9–21, 2013.
- Deek, A., Emeis, K., and van Beusekom, J.: Nitrogen removal in coastal sediments of the German Wadden Sea, *Biogeochemistry*, 108, 467–483, 2011.
- Emeis, K.-C., van Beusekom, J., Callies, U., Ebinghaus, R., Kannen, A., Kraus, G., Kröncke, I., Lenhart, H., Lorkowski, I., Matthias, V., Möllmann, C., Pätsch, J., Scharfe, M., Thomas, H., Weisse, R., and Zorita, E.: The North Sea – A shelf sea in the Anthropocene, *J. Mar. Syst.*, 141, 18–33, 2015.
- Granger, J. and Sigman, D. M.: Removal of nitrite with sulfamic acid for nitrate N and O isotope analysis with the denitrifier method, *Rapid Commun. Mass Sp.*, 23, 3753–3762, 2009.
- Grasshoff, K., Kremling, K., and Ehrhardt, M.: *Methods of Seawater Analysis*, Wiley-VCH, Weinheim, 1–600, 1999.
- Hartmann, M., Müller, P., Suess, E., and Van der Weijden, C. H.: Oxidation of organic matter in recent marine sediments, *Meteor. Forschungs-Ergebnisse, Reihe C*, 74–86, 1973.
- Heip, C. H. R., Goosen, N. K., Herman, P. M. J., Kromkamp, J., Middelburg, J. J., and Soetaert, K.: Production and consumption of biological particles in temperate tidal estuaries, *Oceanogr. Mar. Biol.*, 33, 1–149, 1995.
- Helleman, D., Tallberg, P., and Hietanen, S.: Benthic N_2 production rates, Si cycling and environmental characteristics from the Öre estuary on the Swedish coast, *Mar. Ecol. Prog. Ser.*, 583, 63–80, 2017.
- Henriksen, K. and Kemp, W. M.: Nitrification in Estuarine and Coastal Marine Sediments, in: *Nitrogen Cycling in Coastal Marine Environments*, edited by: Blackburn, T. H. and Sorensen, J., John Wiley & Sons Ltd, SCOPE, 207–249, 1988.
- Hickel, W., Mangelsdorf, P., and Berg, J.: The human impact in the German Bight: Eutrophication during three decades (1962–1991), *Helgoländer Meeresun.*, 47, 243–263, 1993.
- Hydes, D. J., Kelly-Gerrey, B. A., Le Gall, A. C., and Proctor, R.: The balance of supply of nutrients and demands of biological production and denitrification in a temperate latitude shelf sea – a treatment of the southern North Sea as an extended estuary, *Mar. Chem.*, 68, 117–131, 1999.
- Jensen, K. M., Jensen, M. H., and Kristensen, E.: Nitrification and denitrification in Wadden Sea sediments (Konigshafen, Island of Sylt, Germany) as measured by nitrogen isotope pairing and isotope dilution, *Aquat. Microb. Ecol.*, 11, 181–191, 1996.
- Jorgensen, B. B.: Mineralization of organic matter in the sea bed—the role of sulphate reduction, *Nature*, 296, 643–645, 1982.
- Jorgensen, B. B.: Processes at the sediment-water interface, in: *The Major Biogeochemical Cycles and Their Interactions*, edited by: Bolin, B. and Cook, R. B., John Wiley, New York, 477–515, 1983.
- Kana, T. M., Darkangelo, C., Hunt, M. D., Oldham, J. B., Bennett, G. E., and Cornwell, J. C.: Membrane Inlet Mass Spectrometer for Rapid High-Precision Determination of N_2 , O_2 , and Ar in Environmental Water Samples.pdf, *Anal. Chem.*, 66, 4166–4170, 1994.
- Kérouel, R. and Aminot, A.: Fluorimetric determination of ammonia in sea and estuarine water by direct segmented flow analysis, *Mar. Chem.*, 57, 265–275, 1997.
- Koike, I. and Hattori, A.: Simultaneous determinations of nitrification and nitrate reduction in coastal sediments by a ^{15}N dilution technique, *Appl. Environ. Microb.*, 35, 853–857, 1978.
- Krämer, K., Holler, P., Herbst, G., Bratek, A., Ahmerkamp, S., Neumann, A., Bartholoma, A., van Beusekom, J. E. E., Holtappels, M., and Winter, C.: Abrupt emergence of a large pockmark field in the German Bight, southeastern North Sea, *Sci. Rep.*, 7, 5150, <https://doi.org/10.1038/s41598-017-05536-1>, 2017.
- Lenhart, H. J. and Pohlmann, T.: The ICES-boxes approach in relation to results of a North Sea circulation model, *Tellus A*, 49, 139–160, 1997.
- Lohse, L., Malschaert, J. F. P., Slomp, C. P., Helder, W., and van Raaphorst, W.: Nitrogen cycling in the North Sea sediments: interaction of denitrification and nitrification of offshore and coastal areas, *Mar. Ecol. Prog. Ser.*, 101, 283–296, 1993.
- LOICZ: *Land-Ocean Interactions in the Coastal Zone*, 1–215, 1995.
- Los, F. J., Troost, T. A., and Van Beek, J. K. L.: Finding the optimal reduction to meet all targets – Applying Linear Programming with a nutrient tracer model of the North Sea, *J. Mar. Syst.*, 131, 91–101, 2014.
- Marchant, H. K., Holtappels, M., Lavik, G., Ahmerkamp, S., Winter, C., and Kuypers, M. M. M.: Coupled nitrification-denitrification leads to extensive N loss in subtidal permeable sediments, *Limnol. Oceanogr.*, 61, 1033–1048, 2016.
- Neubacher, E. C., Parker, R. E., and Trimmer, M.: Short-term hypoxia alters the balance of the nitrogen cycle in coastal sediments, *Limnol. Oceanogr.*, 56, 651–665, 2011.
- Neumann, A.: Elimination of reactive nitrogen in continental shelf sediments measured by membrane inlet mass spectrometry, PhD, Department Geowissenschaften, Universität Hamburg, Hamburg, 1–152, 2012.
- Neumann, A., van Beusekom, J. E. E., Eisele, A., Emeis, K.-C., Friedrich, J., Kröncke, I., Logemann, E. L., Meyer, J.,

- Naderipour, C., Schückerl, U., Wrede, A., and Zettler, M.: Elucidating the impact of macrozoobenthos on the seasonal and spatial variability of benthic fluxes of nutrients and oxygen in the southern North Sea, in preparation, 2020.
- Neumann A., Möbius J., Hass H. C., Puls W., and Friedrich J.: Empirical model to estimate permeability of surface sediment in the German Bight (North Sea), *J. Sea Res.*, 127, 36–45, 2016.
- Neumann, A., van Beusekom, J. E. E., Holtappels, M., and Emeis, K.-C.: Nitrate consumption in sediments of the German Bight (North Sea), *J. Sea Res.*, 127, 26–35, 2017.
- Nishio, T., Komada, M., Arao, T., and Kanamori, T.: Simultaneous determination of transformation rates of nitrate in soil, *JARQ-Jpn. Agr. Res. Q.*, 35, 11–17, 2001.
- OSPAR: Quality Status Report, London, 176 pp., 2010.
- Pätsch, J. and Lenhart, H.-J.: Daily loads of nutrients, total alkalinity, dissolved inorganic carbon and dissolved organic carbon of the European continental rivers for the years 1977–2002, in: *Berichte aus dem Zentrum für Meeres- und Klimaforschung, Reihe B: Ozeanographie*, University of Hamburg, Germany, 1–159, 2004.
- Redfield, A. C.: The biological control of chemical factors in the environment, *Am. Sci.*, 46, 205–221, 1958.
- Rysgaard, S., Risgaard-Petersen, N., and Sloth, N. P.: Nitrification, denitrification and nitrate ammonification in two coastal lagoons in Southern France, *Hydrobiologia*, 329, 133–141, 1996.
- Sanders, T., Schöl, A., and Dähnke, K.: Hot spots of nitrification in the Elbe Estuary and their impact on nitrate regeneration, *Estuar. Coast.*, 41, 128–138, 2018.
- Seitzinger, S. P. and Giblin, A. E.: Estimating denitrification in North Atlantic continental shelf sediments, *Biogeochemistry*, 35, 235–260, 1996.
- Sigman, D. M., Casciotti, K. L., Andreani, M., Barford, C., Galanter, M., and Böhlke, J. K.: A bacterial method for the nitrogen isotopic analysis of nitrate in seawater and freshwater, *Anal. Chem.*, 73, 4145–4153, 2001.
- Thibodeau, B., Lehmann, M. F., Kowarzyk, J., Mucci, A., Gélinas, Y., Gilbert, D., Maranger, R., and Alkhatib, M.: Benthic nutrient fluxes along the Laurentian Channel: Impacts on the N budget of the St. Lawrence marine system, *Estuar. Coast. Shelf S.*, 90, 195–205, 2010.
- Van Beusekom, J., Brockmann, U. H., Hesse, K.-J., Hickel, W., Poremba, K., and Tillmann, U.: The importance of sediments in the transformation and turnover of nutrients and organic matter in the Wadden Sea and German Bight, *German Journal of Hydrography*, 51, 245–266, 1999.
- van Leeuwen, S. M., van der Molen, J., Ruardij, P., Fernand, L., and Jickells, T.: Modelling the contribution of deep chlorophyll maxima to annual primary production in the North Sea, *Biogeochemistry*, 113, 137–152, 2013.
- von Westernhagen, H., Hickel, W., Bauerfeind, E., Niermann, U., and Kröncke, I.: Sources and effects of oxygen deficiencies in the south-eastern North Sea, *Ophelia*, 26, 457–473, 1986.
- Zhang, L., Altabet, M. A., Wu, T., and Hadas, O.: Sensitive Measurement of $\text{NH}_4^+^{15}\text{N}/^{14}\text{N}$ ($\delta^{15}\text{NH}_4^+$) at Natural Abundances Levels in Fresh and Saltwaters, *Anal. Chem.*, 79, 5297–5303, 2007.